

Electronic Supplementary Information (ESI)

for

Predicting and parameterizing the glass transition temperature of atmospheric organic aerosol components via molecular dynamics simulations

Panagiota Siachouli,^{a,b} Vlasios G. Mavrantzas^{*,a,b,c} and Spyros N. Pandis^{*,a,b}

^aDepartment of Chemical Engineering, University of Patras, Patras, GR 26504, Greece

^bInstitute of Chemical Engineering Sciences (ICE-HT/FORTH), Patras, GR 26504, Greece

^cParticle Technology Laboratory, Department of Mechanical and Process Engineering, ETH Zürich, Zürich CH-8092, Switzerland

S1. T_g predictions from MD simulations

Table S1: MD predictions for the T_g of all compounds. Values from the two methods (density and energy of non-bonded potential energy as a function of temperature) implemented to predict T_g and comparison with available experimental data.

Compound	T_g (K) based on density	T_g (K) based on non-bonded potential energy	T_g (K) experimental
1-propanol	118.2 ± 0.4^1	118.5 ± 6.5^1	100 ± 7^2
2-propanol	130.2 ± 0.4^1	130.9 ± 1^1	119.4 ± 4^2
1,2-propanediol	171.2 ± 4.6^1	180 ± 0.5^1	170 ± 3^2
1,3-propanediol	175.9 ± 3.8^1	178.4 ± 0.3^1	148 ± 8^2
1,2,3-propanetriol	216.2 ± 6.5^1	218.9 ± 5.8^1	189 ± 7^2
1-hexanol	149.6 ± 7.1^1	150.7 ± 0.8^1	N/A
1,6-hexanediol	242.4 ± 5.7^1	242.2 ± 7.1^1	N/A
1,2,6-hexanetriol	258.3 ± 13.4^1	257.9 ± 9.2^1	204 ± 6^2
1-nonanol	167.3 ± 2.2	168.5 ± 0.5	153^2
1,2-nonanediol	251.6 ± 4.6	248.7 ± 12.1	N/A
1,2,9-nonanetriol	264.4 ± 0.5	266.1 ± 1.6	N/A
1-dodecanol	187.6 ± 1.4	185.3 ± 2.1	N/A
1,2-dodecanediol	259.4 ± 2.3	266.9 ± 1.3	N/A
cyclohexanol	173.5 ± 0.6	173.8 ± 0.6	161^3
cyclohexanediol	271.4 ± 5.5	273.7 ± 6.1	N/A
cyclohexanetriol	285.8 ± 1.2	286.4 ± 0.8	N/A
cyclononanol	186.3 ± 1.8	190.3 ± 0.35	N/A
Propionic acid	159.6 ± 5.9^1	160.6 ± 6.2^1	N/A
Malonic acid	275.3 ± 2^1	271.7 ± 0.6^1	N/A
Hexanoic acid	183.2 ± 7.2^1	183.3 ± 8^1	N/A
Adipic acid	280.2 ± 12.2^1	278.8 ± 11.9^1	N/A
Tricarballic acid	316.2 ± 1.1^1	314.2 ± 0.5^1	N/A
Suberic acid	303.4 ± 3.9^1	290.5 ± 0.7^1	N/A
Dimethylsuccinic acid	312.1 ± 3.6^1	312.3 ± 2.7^1	N/A

Dimethylhexanedioic acid	297.3 ± 1.7^1	296.5 ± 1.4^1	N/A
Cyclobutanedicarboxylic acid	315.9 ± 6.2^1	309.5 ± 0.6^1	N/A
Norpinic acid	320.7 ± 0.7^1	320.4 ± 1^1	N/A
3-methyl-1,2,3-butanedicarboxylic acid	336.7 ± 6.7^1	351.2 ± 11.1^1	305 ± 2^4
Nonanoic acid	195.3 ± 6.9	201.6 ± 0.8	N/A
Azelaic acid	302.1 ± 1.3	303.5 ± 1.7	N/A
Dodecanoic acid	200 ± 3.4	204.1 ± 1.1	N/A
Dodecanedioic acid	316.3 ± 3.1	$295.3 \pm .6$	N/A
Cyclopentanedicarboxylic acid	215.6 ± 1.7	$212. \pm 12$	N/A
Cycloheptanedicarboxylic acid	242.4 ± 1.7	243.9 ± 1.2	N/A
2-propanone	112 ± 0.45	108.8 ± 1.9	100^3
Propanal	105.5 ± 1.8	104.7 ± 0.4	N/A
2-hexanone	133.9 ± 1.4	133.6 ± 0.9	N/A
Hexanal	122.9 ± 0.5	122.6 ± 1.3	N/A
2-Nonanone	165.6 ± 0.3	163.3	N/A
Nonanal	157.2 ± 0.5	152.2 ± 2.4	N/A
Diacetyl	162.6 ± 4.9	155.2 ± 3.3	N/A
Cyclopropanone	118.3 ± 0.8	106.5 ± 0.9	N/A
Cyclohexanone	161.3 ± 2	153.8 ± 1.2	N/A
Cyclononanone	181.3 ± 1	181.6 ± 1.1	N/A
Pyruvic acid	192.6 ± 2.6	192.9 ± 1.9	N/A
5-Oxohexanoic acid	205.3 ± 0.9	204.8 ± 1.1	N/A
6-Oxononanoic acid	225 ± 1.4	227.1 ± 0.2	N/A
Oxomalonic acid	285.7 ± 2.1	286.1 ± 4.2	N/A
2-Oxoadipic acid	294.2 ± 3.4	286.3 ± 0.4	N/A
Lactic acid	213.2 ± 11.8	220.8 ± 2.52	207 ± 18^2
Tartronic acid	288.4 ± 2.7	288.2 ± 2.9	N/A
Hydroxy acetone	162.4 ± 2.5	163 ± 1	N/A
Dihydroxy acetone	206.3 ± 3	305.9 ± 1.3	N/A
Cis-pinonic acid	255.1 ± 2.2^1	255 ± 0.9^1	N/A
Pinonaldehyde	185.1 ± 1.9^1	184.7 ± 2.2^1	N/A

S2. Effect of molecular weight and O:C ratio per category of compounds

A) Carbonyls

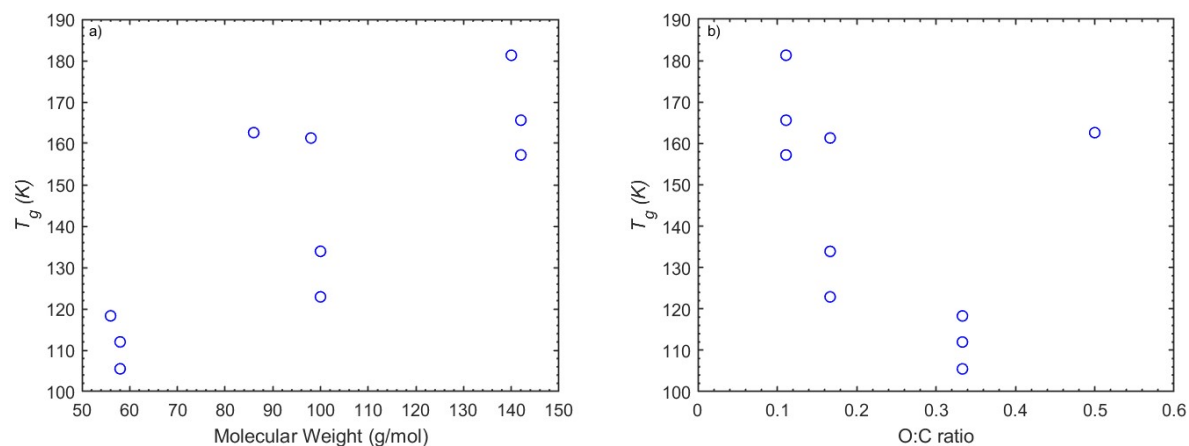


Figure S1: T_g as a function of molecular weight (a) and O:C ratio (b) for the carbonyls.

B) Hydroxyls

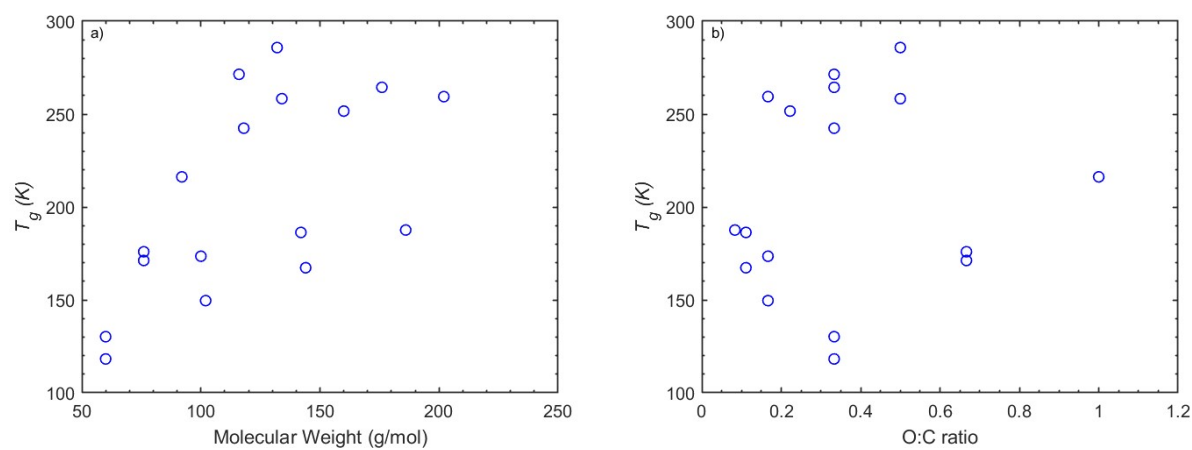


Figure S2: T_g as a function of molecular weight (a) and O:C ratio (b) for the hydroxyls.

C) Carboxyls

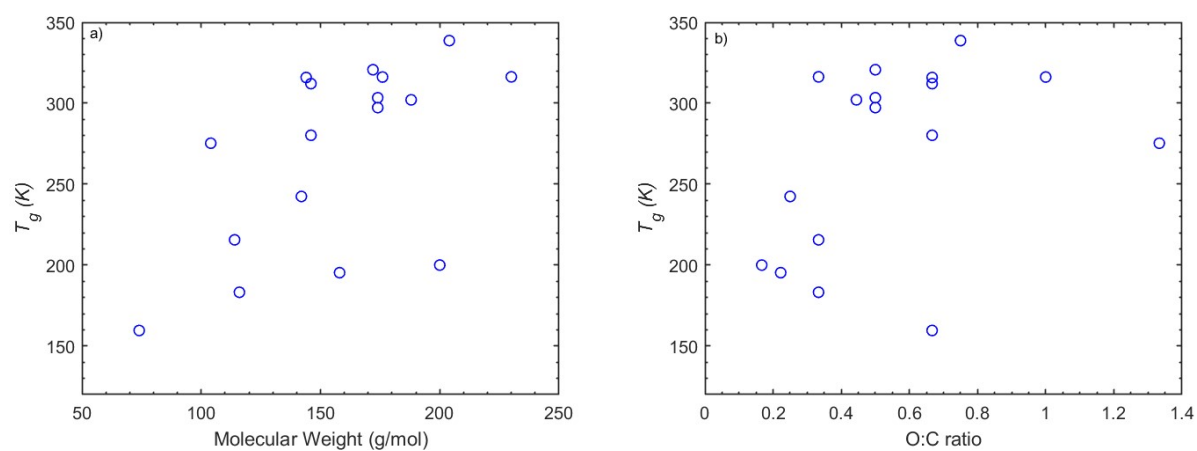


Figure S3: T_g as a function of molecular weight (a) and O:C ratio (b) for the carboxyls.

D) Multifunctionals

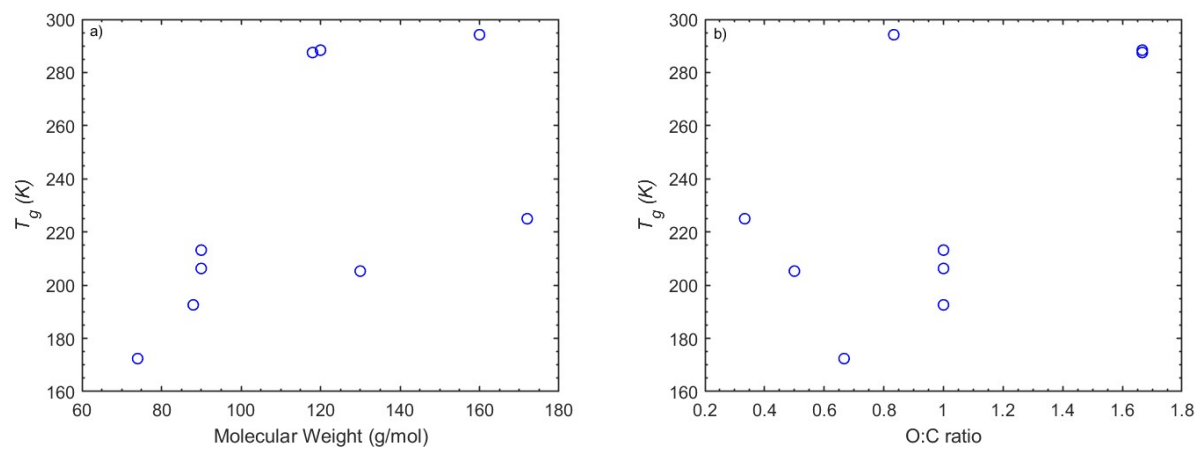


Figure S4: T_g as a function of molecular weight (a) and O:C ratio (b) for the multifunctional compounds.

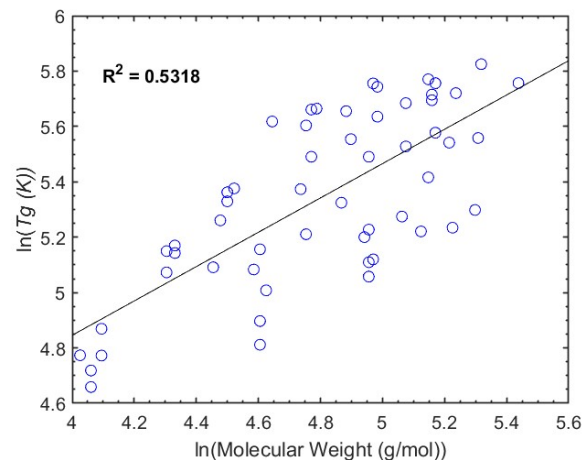


Figure S5: Correlation of the glass transition temperature (T_g) with the molecular weight (M) for the entire dataset. The MD data have been fitted with a power-law of the form $T_g \propto M^\alpha$ as suggested by Novikov and Rössler (2013)⁵ and the best fitting has been obtained for $\alpha = 0.62$.

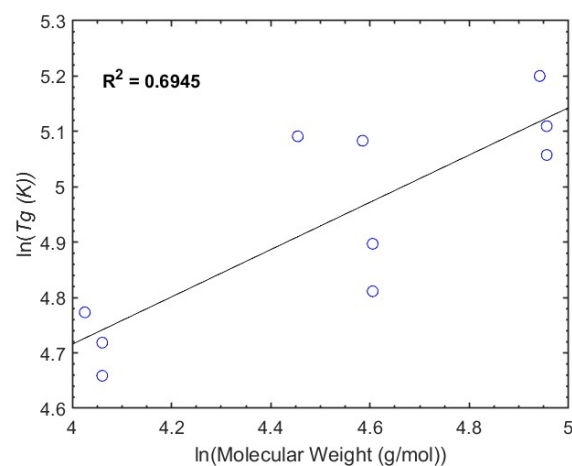


Figure S6: Correlation of the glass transition temperature (T_g) with the molecular weight (M) for the carbonyls. The MD data have been fitted with a power-law of the form $T_g \propto M^\alpha$ as suggested by Novikov and Rössler (2013)⁵ and the best fitting has been obtained for $\alpha = 0.42$.

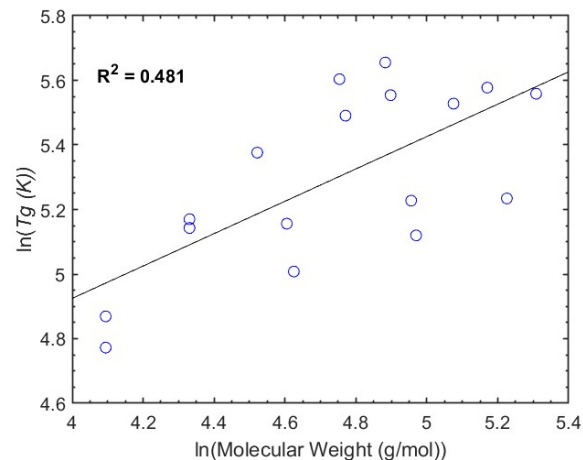


Figure S7: Correlation of the glass transition temperature (T_g) with the molecular weight (M) for the alcohols. The MD data have been fitted with a power-law of the form $T_g \propto M^\alpha$ as suggested by Novikov and Rössler (2013)⁵ and the best fitting has been obtained for $\alpha = 0.50$.

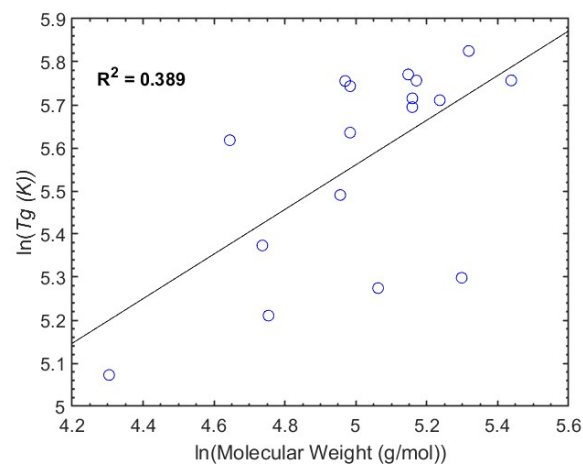


Figure S8: Correlation of the glass transition temperature (T_g) with the molecular weight (M) for the carboxylic acids. The MD data have been fitted with a power-law of the form $T_g \propto M^\alpha$ as suggested by Novikov and Rössler (2013)⁵ and the best fitting has been obtained for $\alpha = 0.51$.

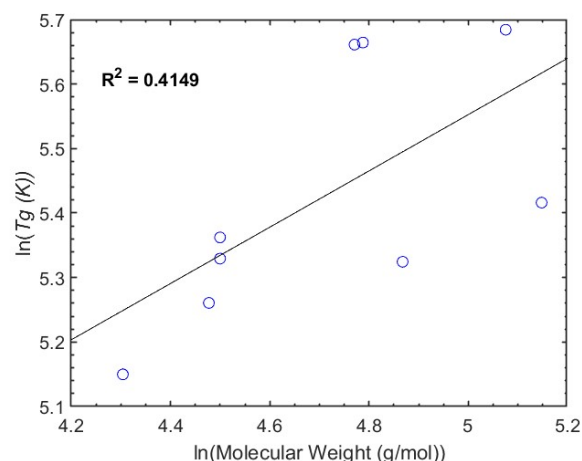


Figure S9: Correlation of the glass transition temperature (T_g) with the molecular weight (M) for the multifunctional organic compounds. The MD data have been fitted with a power-law of the form $T_g \propto M^a$ as suggested by Novikov and Rössler (2013)⁵ and the best fitting has been obtained for $a = 0.43$.

S3. Evaluation of the sensitivity of dataset

To investigate the robustness and sensitivity of our parameterization we examine the variation of the contribution factors. The variation is examined using the leave-one-out scenario, in which we remove all the datapoints once and examine the change in the contribution for each factor considered.

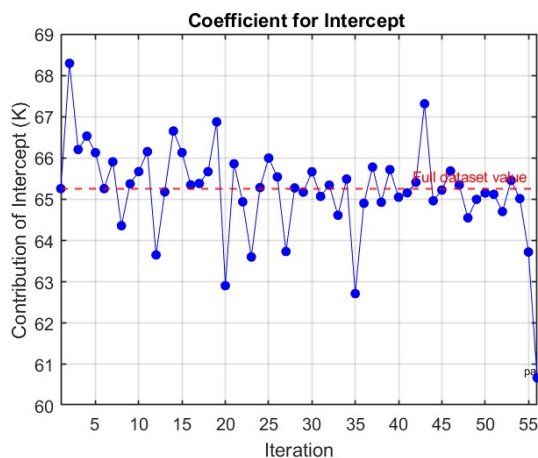


Figure S10: Variation of the intercept's contribution in a leave-one-out scenario with a 5% tolerance threshold. The annotated compounds are those whose removal causes the intercept to deviate by more than 5%.

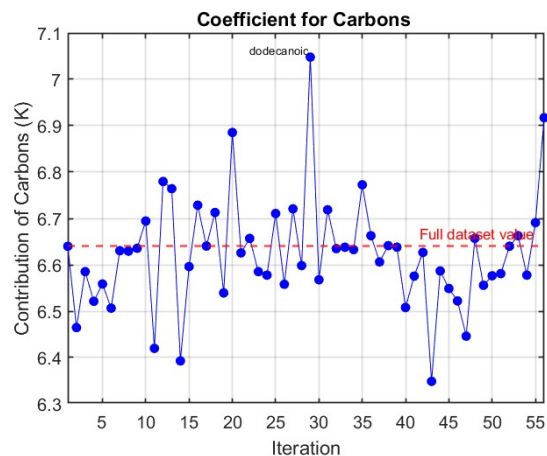


Figure S11: Variation of the intercept's contribution in a leave-one-out scenario with a 5% tolerance threshold. The annotated compounds are those whose removal causes the contribution of carbons to deviate by more than 5%.

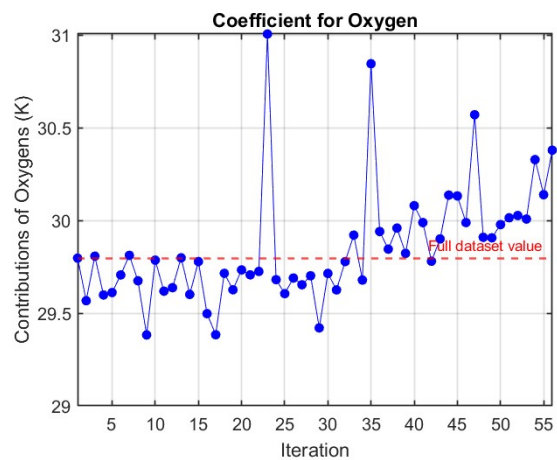


Figure S12: Variation of the intercept's contribution in a leave-one-out scenario with a 5% tolerance threshold. The annotated compounds are those whose removal causes the contribution of oxygens to deviate by more than 5%.

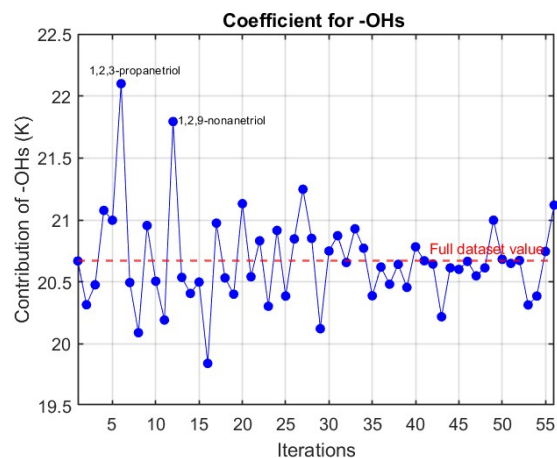


Figure S13: Variation of the intercept's contribution in a leave-one-out scenario with a 5% tolerance threshold. The annotated compounds are those whose removal causes the contribution of hydroxyls to deviate by more than 5%.

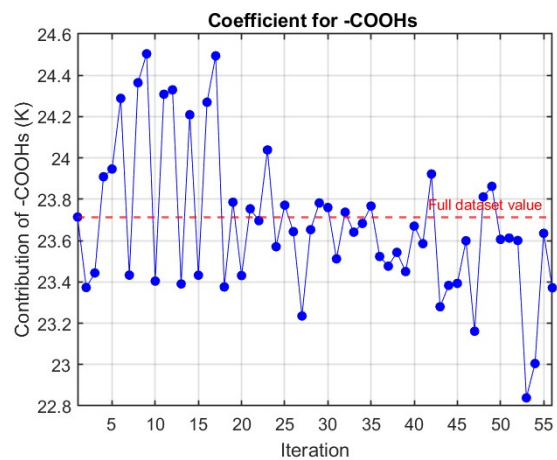


Figure S14: Variation of the intercept's contribution in a leave-one-out scenario with a 5% tolerance threshold. The annotated compounds are those whose removal causes the contribution of carboxyls to deviate by more than 5%.

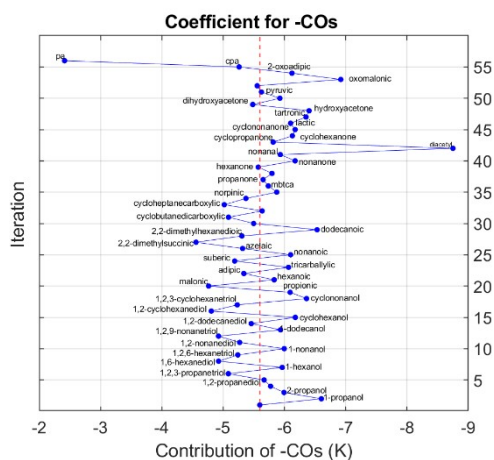


Figure S15: Variation of the intercept's contribution in a leave-one-out scenario with a 5% tolerance threshold. The annotated compounds are those whose removal causes the contribution of carbonyls to deviate by more than 5%.

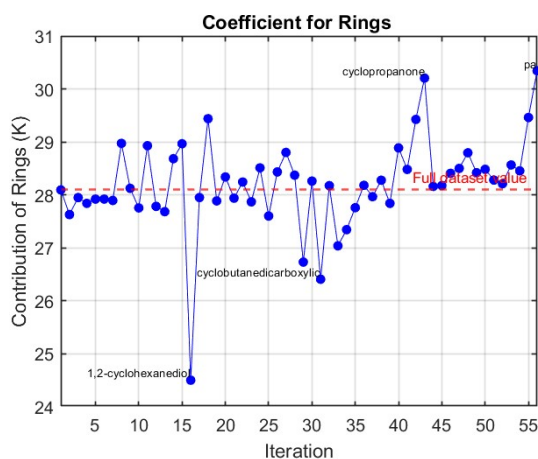


Figure S16: Variation of the intercept's contribution in a leave-one-out scenario with a 5% tolerance threshold. The annotated compounds are those whose removal causes the contribution of rings to deviate by more than 5%.

S4. Estimating the Glass Transition Temperature using the VFT equation

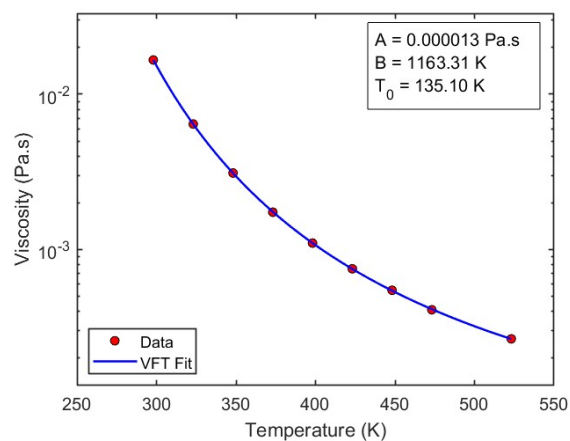


Figure S17: Indirect estimation of the T_g of 1-dodecanol by fitting the viscosity data of Fu et al.⁶ with the VFT equation, Eq. (2) in the main text.

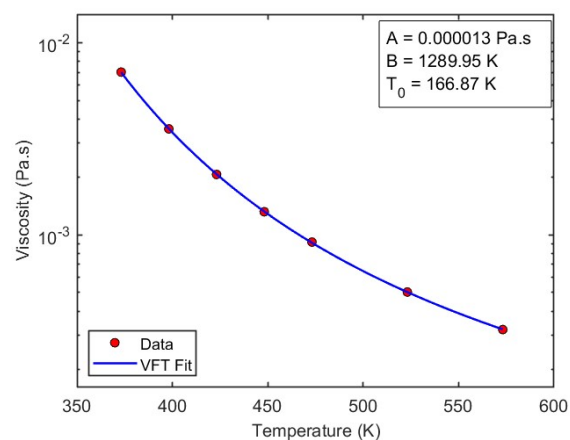


Figure S18: Indirect estimation of the T_g of 1,12-dodecanediol by fitting the viscosity data of Fu et al.⁶ with the VFT equation, Eq. (2) in the main text.

S5. Comparison with other parameterizations

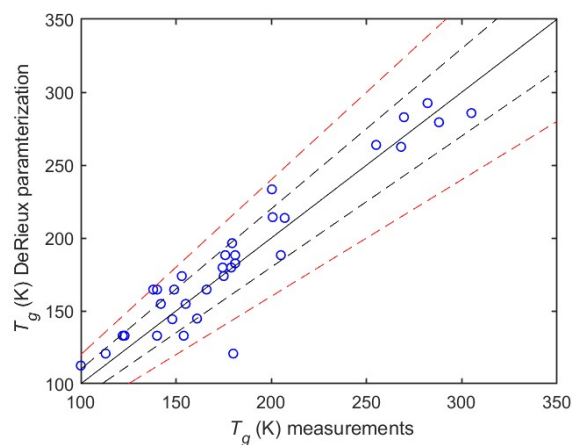


Figure S19: Comparison of the DeRieux et al.⁷ parametrization against measurements. The solid line is the 1:1 curve while the dashed black line indicates the $\pm 10\%$, and the dashed red line represents the $\pm 20\%$ deviations from 1:1.

References

- 1 P. Siachouli, K. S. Karadima, V. G. Mavrantzas and S. N. Pandis, *Soft Matter*, 2024, **20**, 4783–4794.
- 2 N. E. Rothfuss and M. D. Petters, *Environ. Sci. Technol.*, 2017, **51**, 271–279.
- 3 C. A. Angell, J. M. Sare and E. J. Sare, *J. Phys. Chem.*, 1978, **82**, 2622–2629.
- 4 H. P. Dette, M. Qi, D. C. Schröder, A. Godt and T. Koop, *J. Phys. Chem. A*, 2014, **118**, 7024–7033.
- 5 V. N. Novikov and E. A. Rössler, *Polymer (Guildf.)*, 2013, **54**, 6987–6991.
- 6 Y. Fu, X. Meng, X. Liang and J. Wu, *J. Chem. Eng. Data*, 2021, **66**, 712–721.
- 7 W. S. W. DeRieux, Y. Li, P. Lin, J. Laskin, A. Laskin, A. K. Bertram, S. A. Nizkorodov and M. Shiraiwa, *Atmos. Chem. Phys.*, 2018, **18**, 6331–6351.